High-Velocity Impact Behavior of Glass Fiber-Reinforced Polyester Filled with Nanoclay

Javad Moftakharian Esfahani, Masoud Esfandeh, Ali Reza Sabet

Department of Composite, Iran Polymer and Petrochemical Institute, Tehran, Islamic Republic of Iran

Received 30 January 2011; accepted 25 November 2011
DOI 10.1002/app.36605
Published online 2 February 2012 in Wiley Online Library (wileyonlinelibrary.com).

ABSTRACT: This study investigates the effects of nanoclay particles on impact and flexural properties of glass fiber-reinforced unsaturated polyester (UP) composites. UP-reinforced nanocomposite containing 1.5 and 3 wt % nanoclay was used to manufacture laminated composite panels using glass fiber woven roving by hand lay-up method. X-ray diffraction and transmission electron microscopy analysis confirmed intercalation and exfoliation of the nanoclay in the UP resin. Flexural test results indicated better performance for the specimens containing 1.5 wt % nanoclay reinforcements. However, Izod impact test results showed a decrease with increase in nanoclay content. High-velocity impact tests were carried out on a gas gun in velocity range of 90–220 m/s using harden steel hemispherical tip projectile. Highest performance in ballistic limit and energy absorption were obtained for specimens containing 1.5 wt % nanoclay. © 2012 Wiley Periodicals, Inc. J Appl Polym Sci 125: E583–E591, 2012

Key words: nanocomposites; impact behavior; unsaturated polyester; fiber glass; polymer

INTRODUCTION

Fiber-reinforced polymer matrix composites due to their high specific strength and stiffness have been widely used in aircraft, marine, and automotive structures.[1] Incorporation of organo-modified layered silicates (nanoclay) into the polymer matrices has shown potentials for property enhancements including decrease in gas/liquid permeability and increase in heat as well as flame resistance.[2–4] This is mostly attributed to the nanometer scale and high aspect ratio characteristics of the individual platelets.[5] Complete exfoliation of layered silicates is the desired morphology to achieve better barrier properties.[5] In addition, the surface chemistry of nanoclays, processing conditions, and the extent of nanoclay dispersion are important parameters affecting the physical and mechanical properties of polymer-layered silicate nanocomposites.[6–11]

Kornmann et al.[11] reported increase in flexural strength of glass fiber-reinforced polymer composite laminates using nanoclay/epoxy matrix system. Mechanical and thermal properties of noncrimp glass fiber-reinforced clay/epoxy polymer nanocomposites were investigated by Bozkurtthe et al.[12] Their result showed that clay loading has minor effect on the tensile properties. They also reported flexural properties of laminates were improved by clay addition.

Correspondence to: A. R. Sabet (A.Sabet@ippi.ac.ir).

Journal of Applied Polymer Science, Vol. 125, E583–E591 (2012)

The effects of nanoclay particles on flexural and thermal properties of woven carbon fiber-reinforced polymer matrix composites was investigated by Chowdhury et al.[13] They showed that nanoclay addition at low concentrations increased the flexural properties and thermal stability of the polymer composites. Subramaniyan and Sun[14] reported that addition of nanoclay increased the compressive strength of glass fiber reinforced polymer composites fabricated with stitched unidirectional E-glass fibers and an epoxy vinyl ester resin.

Siddiqui[15] studied the mechanical properties of carbon fiber-reinforced plastics (CFRPs) containing organoclay in the epoxy matrix. His finding showed that inclusion of nanoclay led to improvement in flexural modulus of CFRPs. He also reported both the initiation and propagation values for the mode-I interlaminar fracture toughness of CFRP composites increased with increasing clay concentration.

Haque et al.[16] reported significant improvements in mechanical and thermal properties of conventional fiber-reinforced polymer composites with low organo silicate nanoparticles loading.

One of the great concerns about fiber reinforcement polymer composites is the behavior of these materials toward both low- and high-velocity impact loading. There are limited reports on the effect of nanoclay on the low-velocity impact behavior of FRP materials.

Avila et al.[17] investigated the influence of nanoclay on glass-fiber-epoxy polymer-laminated composites under low-velocity impact by falling weight test. The result showed an increase in energy

absorption with addition of 5% nanoclay in a glass fiber/epoxy-laminated composites.

Hosur et al.[18] studied sandwich panels with neat and nanoclay filled foam cores and epoxy–nanoclay polymer composite face sheets. Low-velocity impact response of the samples were recorded and compared. The study revealed samples with nanoclay foam sustained higher loads and had lower damage areas compared with neat counterparts. Nanoclay foam cores also exhibited brittle fracture resistance.

There are many different parameters that influence high-velocity impact behavior of fiber-reinforced polymer composites; these have been thoroughly reviewed by other researchers.[19,20] These parameters include fiber reinforcement, matrix, laminate thickness, impact velocity, and incorporation of secondary reinforcements, for example, nanoparticles.

Among these parameters, the roles of laminate thickness, fiber reinforcement properties, matrix properties, and initial impact velocity have been investigated in great extend.[21–23] These include work by Csukat[21] who investigated the impact performance of different polymer composite material. Csukat demonstrated that the elasticity of matrix greatly affected the energy absorption capacity of polymer composites structure. Cheeseman and Bogetti[22] conducted a study on the effect of impact velocity, material properties, and projectile geometry on ballistic performance of polymer composite laminate. Gellert et al.[23] carried out high-velocity impact test on glass fiber-reinforced plastic composite plates of various thicknesses. However, no report was found in open literature on high-velocity impact behavior of polymer composite containing nanoclay particles.

Therefore, it was decided to look in to the effect of nanoscale size secondary reinforcement in a laminated system under low- and high-velocity impact loading.

EXPERIMENTAL

Materials

E-glass woven roving cloth with areal density of 400 g/m^2 used as reinforcement was obtained from Camelyaf, Gebze Kocaeli Turkey and the Unsaturated polyester (UP) resin (BUSHPOL 751129) with 40 wt % styrene as solvent with viscosity of 650 cP used as matrix was supplied by Bushehr Chemical Industry Iran. Nanoclay (Cloisite 30B) is a natural montmorillonite modified with methyl, tallow, bis-2-hydroxyethyl, quaternary ammonium chloride used as organically modified clay. Nanoclay Cloisite 30B has density of 1.98 kg/m^3 and dry particle size of less than 13 μm. Cloisite 30B was obtained from Southern Clay, Texas USA. Methyl ethyl ketone peroxide (MEKP) from Iran. Peroxide and cobalt naphthenate from AKZONOBLE, Amersfoort Netherlands were used as initiator and the accelerator, respectively.

TABLE I
Matrix of Variables for Polymer Nanocomposites Laminates

Code	Number of layers	Nanoclay content (%)	Thickness (mm)	Areal density (g/cm^2)
4H0	4	0	2.14 (0.1)	0.3 (0.03)
4H1.5	4	1.5	2.10 (0.15)	0.29 (0.07)
4H3	4	3	2.3 (0.05)	0.32 (0.05)
8H0	8	0	3.8 (0.2)	0.57 (0.1)
8H1.5	8	1.5	3.85 (0.27)	0.6 (0.08)
8H3	8	3	4.05 (0.32)	0.64 (0.06)
12H0	12	0	5.94 (0.4)	1.004 (0.4)
12H1.5	12	1.5	6.42 (0.51)	1.018 (0.32)
12H3	12	3	6.23 (0.42)	1.014 (0.28)

Preparation of the uncured UP polyester resin-nanoclay

UP resin/nanoclay nanocomposites were prepared through melt-mixing UP resin directly with required amount of Cloisite 30B. For the preparation of samples with 1.5 and 3% wt nanoclay, the nanoclay was placed in an oven for 1 h at 110°C to remove any moisture, and it was then added to UP resin, and mixed using a homogenizer at 8000 rpm for 80 min, to achieve a homogenous mixture.[24,25]

Preparation of the glass fiber-reinforced nanocomposite laminates

Polymer composite specimens were made by hand lay-up method using 400g/m^2 E-glass plain weave woven roving and UP resin/nanoclay in a 150 × 150 mm^2 size as defined by target holder in the high-velocity impact device. MEKP (1 wt %) and cobalt naphthenate (0.1 wt %) were added as curing agent and accelerator. All specimens were cured for 24 h at room temperature and postured for 20 h at 80°C.

The specimens were prepared in 4, 8, and 12 layers, and their thickness varied from 2.1 to 6.4 mm depending on the number of layers and nanoclay percentage. In all, nine different types of hybrid polymer nanocomposite panels were made for testing, see Table I. In this table, the number on the left-hand side in the first column represents number of layers and the number on the right-hand side in the same column represents the percentage of nanoclay content in the laminate. For each type of polymer composite plates, at least three specimens were made and tested. The fiber mass fractions of the laminates based on the nanocomposite polymer matrix were 0.62–0.64. These values were determined by burn-off test method per ASTM D7348, by

placing samples cut from the composite panels in a muffle furnace at 600°C for 90 min.

Characterization and compositional analysis

Morphological study and compositional analysis of specimen were carried out by transmission electron microscopy (TEM) and energy dispersive X-ray analysis (EDXA). Nanostructure of the nanoclay (layered silicate) was also studied using X-ray diffraction (XRD). Rheological study of liquid state UP resin/nanoclay was also conducted by viscosity measurements to investigate state of nanoclay dispersion.[25–27]

TEM was performed on ultramicrotomed sample prepared using a LEICA Microsystem, Milton Keynes UK microtome equipped with a glass knife mounted on 200-mesh copper grids. TEM observation was performed on a LEO 906 using an accelerating voltage of 100 kV.

EDXA was performed by gold coating of cryofractured surface of the samples and using EDXA 32 (Genesis) with accelerating voltage of 20 kV to investigate the distribution of aluminum metal element available on surface of nanoclay layers dispersed in the UP resin.

XRD patterns were obtained using a Philips XPERT XRD system equipped with CuKα radiation source at the generator voltage of 40 kV and generator current of 40 mA ($\lambda = 1.5405$ Å). The XRD specimens were made into powder form and Bragg's law, $\lambda = 2d\sin\theta$, was used to calculate the crystallographic spacing (d-spacing), to show the intercalation and exfoliation of nanoclay in UP resin.

A viscosity change for each sample was measured at room temperature as an alternative method to confirm the intercalation and exfoliation of nanoclay using a Brookfield viscometery, Essex UK type RVD-II + Pro LKI 02.[25–27] Also, to characterize cure content of specimens, differential scanning calorimetry (DSC) study was conducted after 24 h on postcured UP resin with and without nanoclay.[28,29] DSC thermograms were recorded using a Polymer Laboratories-PL-DSC at a heating rate of 10°C/min under an extra dry N_2 atmosphere over a temperature range of 25–300°C.

Mechanical properties

The flexural tests were performed according to ASTM D 792 using universal tensile machine Santam STN-150KN equipped with a three-point bending rig. The vertical displacement speed of the rig during the test was 1 mm/min. Five specimens for each composition were tested.

Izod impact test was carried out based on ASTM D 256, using Zwick impact tester. Also hardness tests were performed according to ASTM D 2583 using Barcol Impressor (GYZJ 934-1) as a measure to control degree of cure in neat UP resin and UP resin nanocomposites. Five specimens for each composition were tested.[30]

High-velocity impact test

High-velocity impact tests were carried out using a gas gun (Figure 1) The gas gun consists of 1.75-m long smooth barrel with inside diameter of 8.7 mm, a fast acting high-pressure release valve, a breech unit, a rupture disk unit, a supply gas vessel, a 500-mL gas reservoir for each shot release, a target holder, two projectile velocity measuring units, and ballistic paste to catch the projectile intact. Initial velocity of projectile was measured after it was propelled from the gun barrel using a chronograph F-1 model from Shooting Chrony, Ontario Canada. Because of unpredictable line of flight of projectile after exiting the target, the residual velocity for the projectile which perforated the specimen was recorded using two sets of wide screen aluminum foil panels connected in series via a 1-GHz counter. The 150 × 150 mm specimen is clamped at all four edges. Further details regarding the set up may be found in Ref. [31]. The projectile used for all high-velocity impact tests were hemispherical tip hardened steel (Rc60) of 26.5-mm total length, 8.7 mm diameter, and 11.54 g weight. Initial velocity of projectile (before impact) was calibrated and measured for helium gas at various gas pressures with a chronograph and depicted in Figure 2. The calibration curve showed nonlinear behavior for various gas pressures versus projectile velocities at high-pressure range. Average of five highest impact velocity tests that caused perforation but were unable to go through (projectile seized in the target) was defined as ballistic limit velocity V_{50} (MIL-STD-662F standard). In full perforation tests, initial impact velocity as well as projectile residual velocity was used to arrive at energy absorption using Eq. (1):

$$E = \frac{m}{2}V_i^2 - \frac{m}{2}V_r^2 \quad (1)$$

where E is the energy absorbed by the specimen, V_i is the Initial impact velocity, V_r is the projectile residual velocity after exiting the composite target, and m is the projectile mass.

RESULTS AND DISCUSSION

Characterization

Transmission electron microscopy analysis

Figure 3 present TEM micrograph for specimen with 1.5% wt nanoclay, in this micrograph, the dark lines

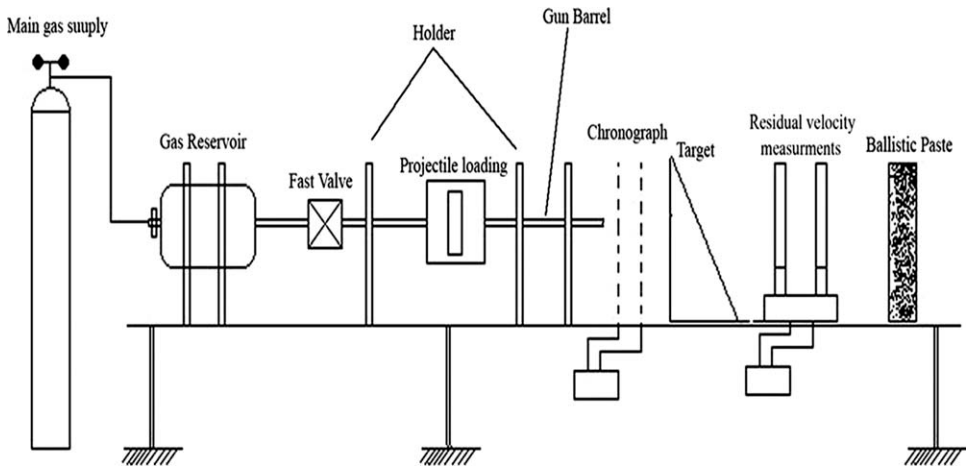

Figure 1 Schematic representation of high-velocity impact testing device (Gas Gun).

are individual silicate layers and white area indicate UP resin. The figure shows clay layers irregularly separated to 10–20 nm with relative exfoliation resulting in well dispersion of polymer nanocomposites. However, for the specimen with 3% wt nanoclay, the interlayer spacing between clay layers is less, indicating intercalations rather than exfoliation of nanoclay. This assertion is supported by EDXA and XRD analysis, to be discussed in the following section. The exfoliation of 1.5% wt nanoclay may be directly attributed to level of nanoclay used and better dispersion as well as less agglomerations in the 1.5% wt as compared to 3% wt nanoclay containing specimens.

EDXA analysis

EDXA compositional analysis was performed on the fracture surface of polymer nanocomposites to show the distribution of aluminum metal element which is available on surface of nanoclay layers in the UP resin. EDXA micrographs of the polymer nanocomposites containing 1.5 and 3 wt % nanoclay are shown in Figure 4(a,b), respectively, where black area is aluminum metal of nanoclay into white template that shows UP resin. In this figure, silicate layers of nanoclay particles were evenly distributed in matrix resin in specimens containing 1.5 and 3 wt % nanoclay, but there are some region containing agglomeration of nanoclay particles in specimen containing 3 wt % nanoclay, for example, shown in Figure 4(b) by the circles.

X-ray diffraction analysis

Figure 5 shows the XRD patterns for UP resin/Cloisite 30B nanocomposites at various clay contents, as compared with Cloisite 30B. For UP resin/Cloisite 30B nanocomposite with 3 wt % Cloisite 30B content, the interlayer spacing has increased from 1.64 nm for the original Cloisite 30B to 3.99 nm ($2\theta = 2/21$), indicating the great extent of intercalation of the Cloisite 30B layers by UP resin, whereas polymer nanocomposites containing 1.5 wt % nanoclay Cloisite 30B showed almost no peaks, indicating an exfoliation of Cloisite 30B in UP resin.

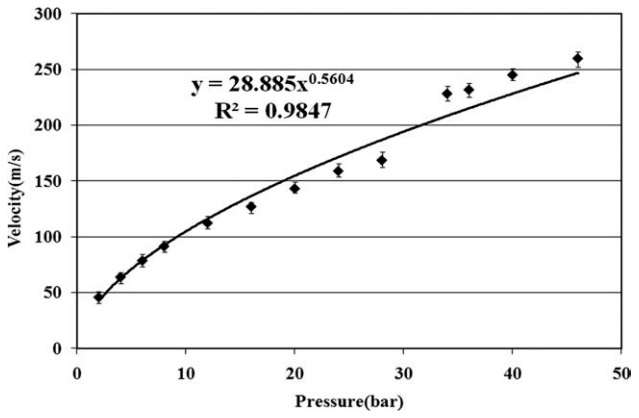

Figure 2 Projectile velocity calibrations for various helium gas pressures.

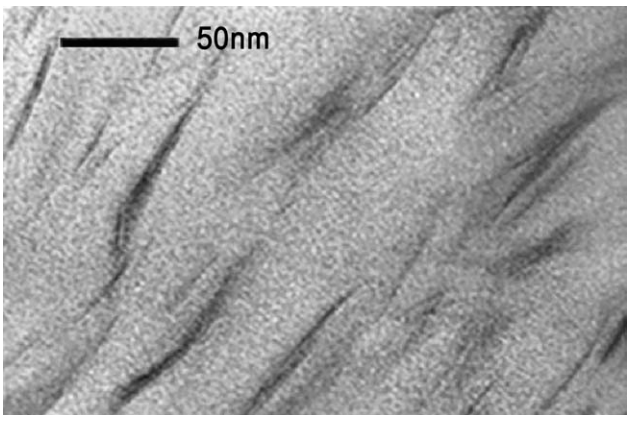

Figure 3 TEM micrographs of polymer nanocomposite with 1.5% wt nanoclay.

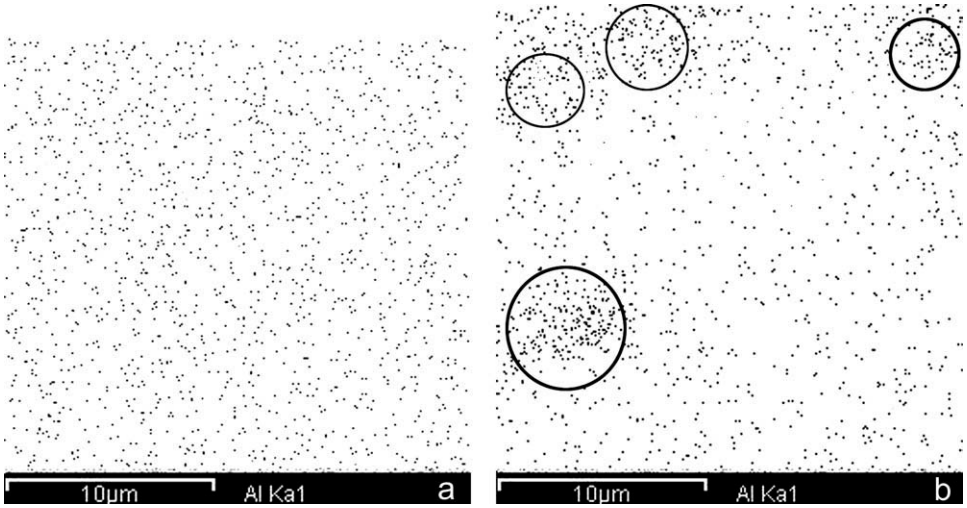

Figure 4 EDXA micrographs of (a) nanocomposite with 1.5% wt nanoclay and (b) nanocomposite with 3% wt nanoclay.

These results show exfoliation and intercalation of polymer nanocomposites containing 1.5 and 3 wt % Cloisite 30B, respectively. This is attributed to strong miscibility between UP resin and Cloisite 30B which originates from strong hydrogen bounding between the carboxyl group of UP resin and hydroxyl group in the gallery of Cloisite 30B.

Viscosity analysis

Table II shows viscosity of neat UP resin and UP resin/nanoclay at 1.5 and 3 wt % nanoclay prepared by mechanical mixing. The result shows a considerable increase in the viscosity of UP resin/nanoclay mixture which utilizes a mechanical stirrer. As shown in Table II, addition of only 1.5 wt % nanoclay into UP resin led to 2.3 time increasing in viscosity of resin. Also, mixing of 3 wt % nanoclay into UP resin led to 2.4 time increase in viscosity. This viscosity increase is related to the increase in the contact surface between the clay and the polymer molecules and the increase of the clay–resin interactions, which causes an increase in resistance to flow, therefore increasing the viscosity. Comparison of viscosities for specimens containing 1.5 and 3 wt % nanoclay indicates exfoliated layers of nanoclay having higher interaction with chains of polymers compared with intercalated layers of nanoclay. The increase in viscosity when compared with the original resin system also signifies the intercalation of the clay particles into the resin mix.

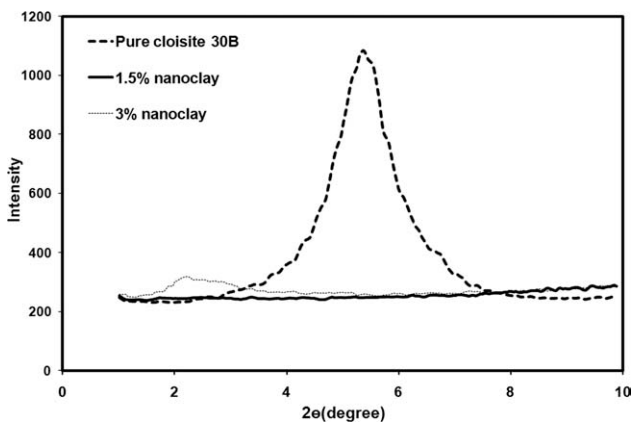

Figure 5 XRD patterns for UP resin/Cloisite 30B polymer nanocomposites and Cloisite 30B.

Curing analysis

DSC curve for the cured UP resin is shown in Figure 6. As it can be seen, there is no exotherm peak in the temperature range 25–300°C, indicating complete curing of the UP resin. This confirms that cure cycle adopted was suitable for complete cure of the specimens.

Physical and mechanical properties

Hardness test

The hardness level of composite laminates is a quantitative parameter which can be used to investigate the degree of crosslink density and curing proportion.[26,30] Hardness test were, therefore, performed on each specimen as a measure to control the degree of cure state. Table II shows the Barcol hardness of

TABLE II
Hardness and Viscosity Measurements of Nanocomposites

Clay content (%)	Viscosity (cP)	Hardness (Barcol)
0	650	66 (13)
1.5	1505	68.4 (16)
3	1560	67.8 (15)

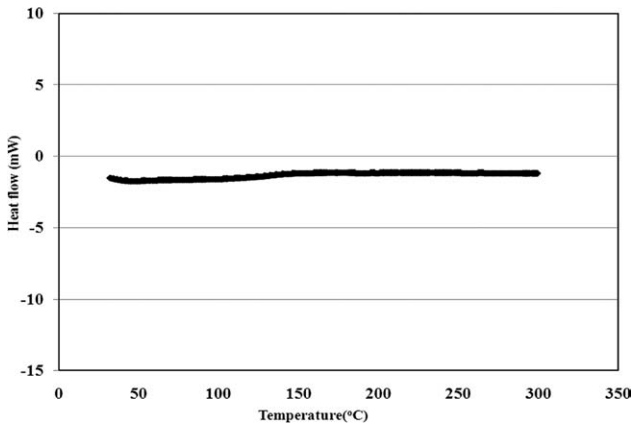

Figure 6 DSC curve of the cured UP resin.

the nanocomposite laminates. This table shows no significant increase in the hardness level of the nanoclay containing specimens indicating same level of cure. The result shows hardness level for 1.5 and 3 wt % nanoclay Cloisite 30B is only increased by 3.6 and 2.7%, respectively, compared with the hardness of the cured neat UP resin. Results confirm that all specimens including 1.5 and 3 wt % containing nanoclay and resin without nanoclay are cured in same condition and level.

Flexural properties

Flexural properties for specimens containing different amount of nanoclay are shown in Table III. The result for flexural modulus and strength showed increase due to the presence of a nanocomposite, similar improvements were reported by Haque et al.[16] The flexural property increase is possibly linked to the fact that the tensile and compressive strength for the polyester matrix is improved by the presence of the layered silicate resulting in improvement in the bending strength of the corresponding fiber reinforced polymer composite. However, slight reduction in flexural modulus for 3% wt clay contents as compared to specimen containing 1.5 wt % is attributed to unwanted agglomerates formation, which in turn reduced the reinforcing efficiency of clay.[16] The formation of agglomerate is also confirmed in EDXA analysis [Fig. 4(b)] as well as XRD results.

TABLE III
Flexural Properties of Polymer Nanocomposites Laminate

Nanoclay content (%)	Flexural modulus (MPa)	Flexural strength (MPa)	Elongation at break (%)
4H0	9571.3 (1561.7)	191.9 (34.8)	3.34 (0.5)
4H1.5	11,383 (1132)	218.5 (43.6)	2.76 (0.3)
4H3	10,761.5 (164.5)	229.8 (10.9)	2.96 (0.3)

Low-velocity impact

The results for low-velocity impact test (Izod impact test) for the specimens with different amount nanoclay 30B are shown in Figure 7. The figure shows decrease of 24.4 and 30.1% in low-velocity impact strength for specimens containing 1.5 and 3 wt % of nanoclay, respectively.

This decrease in Izod impact strength in UP resin/nanoclay/fiber glass has been attributed to number of reasons, one being, the presence of silicate layers of nanoclay in vicinity of fiber reinforcement which reduces fiber and matrix flexibility and results in the brittleness of the nanocomposite laminates. The other reason could be the agglomerated nanoclay may have acted as simple filler which in composite always result in more brittleness of the structure.[11,13] The agglomeration of nanoclay in specimen containing 3 wt % nanoclay led to intensification of this behavior, this has also been reported by Kornmann[11] and Chowdhury.[13] Presence of possible air bubbles due to increased in resin viscosity and difficulty in lay up during laminate construction may be another reason for the decrease in low-velocity impact strength.

High-velocity impact

High-velocity impact performance for each specimen was studied by determining ballistic limit velocity V_{50}. These are depicted in Table IV. To minimize the effect of thickness change in the polymer composite specimens, the ballistic limit values and energy absorption were accordingly normalized by dividing the ballistic limit and energy absorption to thickness of each sample, also presented in Table IV.

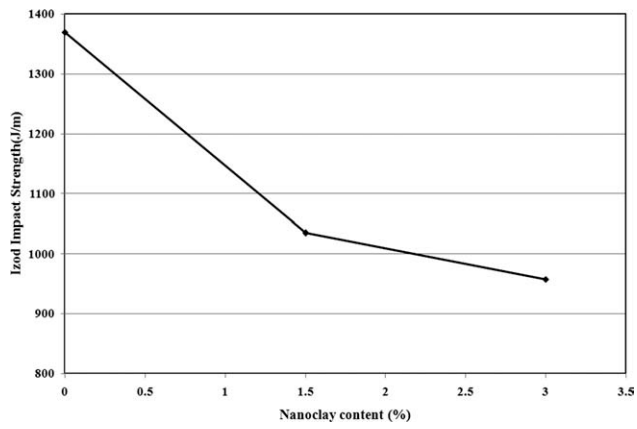

Figure 7 Low-velocity impact strength of composite laminates.

TABLE IV
Ballistic Limit and Energy Absorption Result for Nanocomposite Laminates

Specimen code	Ballistic limit V_{50} (m/s)	Energy absorption at V_{50} (J)	Ballistic limit/thickness ([m/s]/mm)	Ballistic limit/areal density ([m/s]/cm^2)	Energy absorption at V_{50}/ thickness (J/mm)	Energy absorption at V_{50}/areal density ((m/s)/cm^2)
4H0	96 (4)	53.06	44.87	320.07	24.79	176.87
4H1.5	115 (9)	76.02	54.73	396.31	36.20	262.14
4H3	105 (8)	63.58	45.70	328.47	27.64	198.69
8H0	125 (11)	89.73	32.83	218.88	23.61	157.42
8H1.5	157 (15)	142.01	40.77	261.58	36.89	236.68
8H3	135 (13)	104.41	33.23	213.62	25.78	163.14
12H0	174 (15)	174.04	29.28	173.21	29.30	173.35
12H1.5	218 (17)	273.78	33.97	214.25	42.64	268.94
12H3	193.5 (17)	215.48	31.06	190.82	34.59	212.50

Numbers in the brackets are the standard deviation from the mean value for five tests.

Results indicate that the presence of nanoclay improves ballistic limit value compared to specimens containing no nanoclay. The results show specimens with 1.5 wt % nanoclay content attaining highest ballistic limit velocity value for different number of layers.

Figure 8 shows the residual velocity as a function of impact velocity for specimens with 4, 8, and 12 layers. This figure clearly exhibit better ballistic performance for specimen containing nanoclay by showing lower residual velocities for different initial impact velocities.

Results revealed lower residual velocity for specimens with 1.5 and 3 wt % of nanoclay as against specimen without any nanoclay, indicating better energy absorption in these specimens. As discussed earlier, increase in energy absorption in nanoclay containing specimen is possibly linked to the fact that the compressive strength of the laminates is improved by the presence of the nanoclay. On the other hand, existence of nanoclay also increases their flexural strength which consequently results in better energy absorption of the specimens. This can be explained that as the first stage in any high-velocity impact event is in contact, resulting in specimen's compression followed by indentation and penetration, respectively. In this way, compressive strength in the first stage and the flexural strength in the latter two stages play their role in ballistic performance of the structure. Similar findings have also been reported.[12]

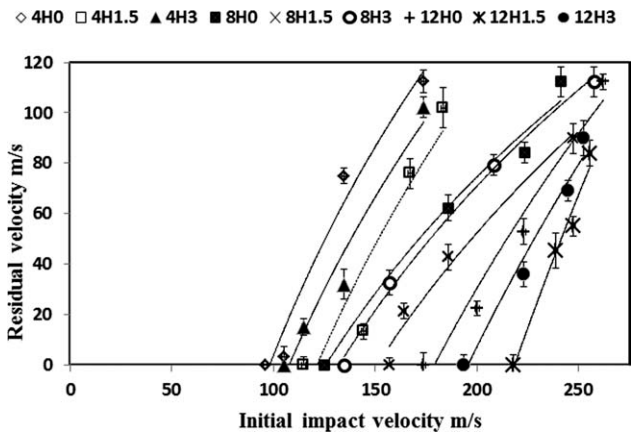

Figure 8 Residual velocity versus initial impact velocity for specimens with 4, 8, and 12 layers.

Improvement in energy absorption may also be because addition of nanoclay led to improvement in interlaminar shear strength as reported by Iqbal[27] which increases delamination resistance of polymer composite, a dominating mechanism in absorption energy of polymer composite laminates during high-velocity impact test, especially, in thick laminates.[22,31]

Also, specimens with 1.5 wt % nanoclay showed maximum energy absorption and decrease in the residual velocity, whereas the specimens with 3 wt % nanoclay indicated reduction in impact strength compared to 1.5 wt % nanoclay samples, this reduction is probably due to poor dispersion of nanoparticles, which acts as stress concentration areas.

Figure 9 shows that V_{50} is a linear increasing function of specimen's thickness regardless of being nanoclay filled or none filled. The figure indicates a relative linear increase in V_{50} with increase in plate thickness for the plates containing fiber reinforcements only. The figure shows that the rate of linear increase for the V_{50} as a function of laminates thickness has highest value for the specimens containing 1.5% nanoclay. As depicted in this figure, increase in thickness plate, leads to increase in the slope of the curve by 23.87 and 22.67 for laminates containing 1.5 and 3% wt nanoclay, respectively, but for laminates

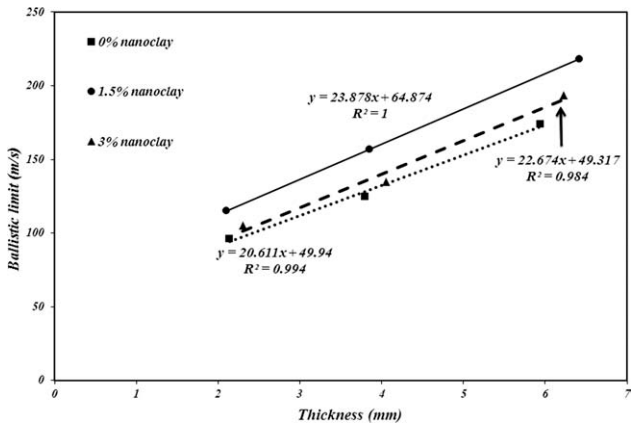

Figure 9 Ballistic limits versus thickness for specimens with different nanoclay contents.

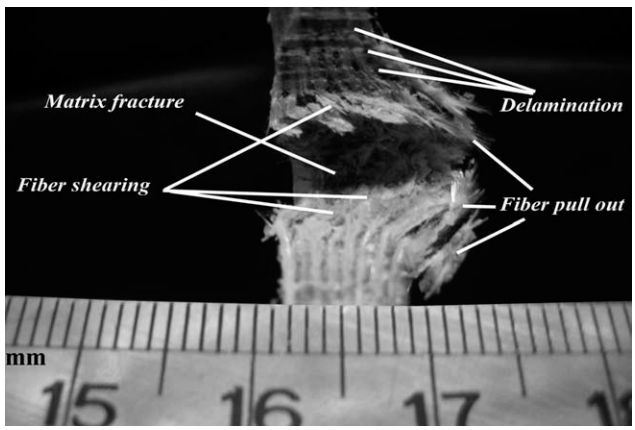

Figure 10 Major energy absorption mechanisms for composite laminates under high-velocity impact.

without nanoclay, the slope of linear increasing rate of ballistic limits values improve by 20.61 as thickness plate increases. It is notable that the value of ballistic limit velocity in specimen with 1.5% wt nanoclay in eight layers is close to the ballistic limit value for the specimen without nanoclay in 12 layers. For laminates containing more layers (higher thickness), the addition of nanoclay especially with good dispersion can synergist the fiber reinforcement effect in nanocomposite laminates. This effect is shown in Figure 9. The figure also shows that linear increasing slope in ballistic limit velocity improves by increasing thickness. Comparison of linear slopes of different specimens shows that in laminates with higher thickness, the effect of well-dispersed nanoclay is more evident in ballistic limit value.

Energy absorption comparison between low-velocity impact Izod test (Fig. 7) and that of high-velocity impact test (Table IV and Fig. 8) reveals rather contradictory results, as low performance were obtained for specimens containing nanoclay as against specimens without it for Izod test whereas in high-velocity impact tests, the result clearly showed better performance for nanoclay containing specimens. This contradiction may be due to number of reasons, including induced stress wave and its propagation, impacting head geometry, mode of loading, strain rates sensitivity, and mode of fracture.

Damage assessment

To predict and recommend sequence of lay up on laminates containing nanoclay particle under high-velocity impact, recognition of major energy absorption mechanisms is necessary. In this part, recognition of major energy absorption mechanisms of polymer nanocomposite laminates has been investigated. In all specimens, regardless of nanoclay content, the failures were mainly of delamination, matrix fracture, fiber shearing, fiber pull out, and fiber fracture as shown in Figure 10. Damage extension area that was mainly through delamination was determined using a back light marking and whitening phenomenon associated with brittle fractures of composite plates. To measure the extension of delamination damage, direct photo scanning of both side of each plate's damage area were carried out using a flat bed scanner at 300 dpi. Damage extension was measured by printing the marked area showing delamination extension followed by cutting out the area and weighing with corresponding unit area. Results are depicted in Figure 11. The study of damage extension associated with thick-walled specimens (12 layered) indicates higher delamination area near the back face in comparison with impacting face. Other failure modes observed were fiber fractures, pull out, and shearing. But in thin specimen (four layers), the delaminated area is much lower than thick

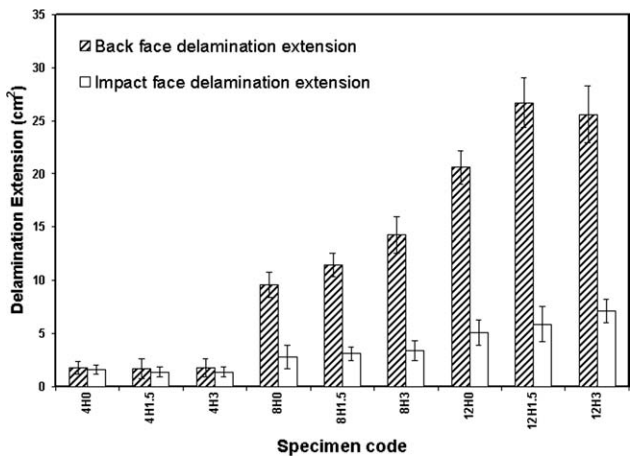

Figure 11 Delamination extension for each specimen.

laminates. From this, one may conclude that delamination being the major energy absorption mechanism in thick specimens.

Figure 11 also shows that in the thin-walled specimens, regardless of nanoclay content, the delamination extension on the back face of the plates are very similar for all specimens, but the delaminated area in thick laminates vary with increase nanoclay content. This difference in delamination area with addition of clay content may be attributed to improvement in interlaminar shear strength by increase in nanoclay content. This justify higher effects of nanoclay particle on linear increasing slope of ballistic limit and energy absorption values as function of laminate thickness presented in the Figure 9.

CONCLUSIONS

The experimental results conducted point out to the following concluding comments.

1. TEM and XRD analysis and viscosity measurements confirmed intercalation and exfoliation of nanoclay particles in UP resin system.
2. Flexural test results indicate improvement in strength and modulus of polymer nanocomposites, with specimen containing 1.5 wt % nanoclay showed highest value, but Izod impact strength of polymer nanocomposite laminates decreased with addition of nanoclay.
3. High-velocity impact result indicated better ballistic performance for specimen containing nanoclay by showing lower residual velocities and energy absorption in particular in exfoliated nanocomposite specimen containing 1.5 wt % nanoclay.
4. High-velocity impact test also indicated relative linear increase in ballistic limit velocity and energy absorption for laminates containing nanoclay with increase in plate thickness.
5. Damage assessments of impact area for all specimens showed delamination as being dominant failures mechanism. Presence of nanoclay played no significant effect in damage extension for thin-walled specimen. However, the delaminated extension in thick laminates varied with increase in nanoclay content.

References

1. Ulven, C.; Vaidya, U.; Hosur, M. Compos Struct 2003, 61, 143.
2. Xu, R.; Manias, E.; Snyder, A.; Runt, J. Macromolecules 2001, 34, 337.
3. Giannelis, E. Adv Mater 1996, 8, 29.
4. McNally, T.; Raymond Murphy, W.; Lew, C.; Turner, R.; Brennan, G. Polymer 2003, 44, 2761.
5. Pavlidou, S.; Papaspyrides, C. D. Prog Polym Sci 2008, 33, 1119.
6. Song, J.; Hsieh, A. Proceedings of the 17th American Society for Composites, Purdue University, west Lafayette, USA, 2002.
7. Nguyen, L. H.; Nguyen, D. T.; La, T. H.; Phan, K. X.; Nguyen, T. T.; Nguyen, H. N. J Appl Polym Sci 2007, 103, 3238.
8. Sharma, S. K.; Nema, A. K.; Nayak, S. K. J Appl Polym Sci 2010, 115, 3463.
9. Nourbakhsh, A.; Ashori, A. J Appl Polym Sci 2009, 112, 1386.
10. Chen, H.; Wang, M.; Lin, Y.; Chan, C. M.; Wu, J. J Appl Polym Sci 2007, 106, 3409.
11. Kornmann, X.; Rees, M.; Thomann, Y.; Necola, A.; Barbezat, M.; Thomann, R. Compos Sci Technol 2005, 65, 2259.
12. Bozkurt, E.; Kaya, E.; Tanoglu, M. Compos Sci Technol 2007, 67, 3394.
13. Chowdhury, F.; Hosur, M.; Jeelani, S. Mater Sci Eng A 2006, 421, 298.
14. Subramaniyan, A.; Sun, C. J Compos Mater 2008, 42, 2111.
15. Siddiqui, N.; Woo, R.; Kim, J.; Leung, C.; Munir, A. Compos A 2007, 38, 449.
16. Haque, A.; Shamsuzzoha, M.; Hussain, F.; Dean, D. J Compos Mater 2003, 37, 1821.
17. Avila, A.; Soares, M.; Silva Neto, A. Int J Impact Eng 2007, 34, 28.
18. Hosur, M.; Mohammed, A.; Zainuddin, S.; Jeelani, S. Compos Struct 2008, 82, 101.
19. Abrate, S. Impact on Composite Structures; Cambridge University Press, Cambridge UK, 1998.
20. Abrate, S. Appl Mech Rev 1994, 47, 517.
21. Faur-Csukat, G. Adv Polym Compos Technol 2006, 239, 217.
22. Cheeseman, B.; Bogetti, T. Compos Struct 2003, 61, 161.
23. Gellert, E.; Cimpoeru, S.; Woodward, R. Int J Impact Eng 2000, 24, 445.
24. Beheshty, M.; Vafayan, M.; Poorabdollah, M. Polym Compos 2009, 30, 629.
25. Pinnavaia, T. J.; Beall, G. W. Eds. Polymer–Clay Nanocomposites; Wiley: New York, 2000.
26. Krishnamoorti, R.; Vaia, R. A.; Giannelis, E. P. Chem Mater 1996, 8, 1728.
27. Iqbal, K.; Khan, S.; Munir, A.; Kim, J. Compos Sci Technol 2009, 69, 1949.
28. Janq, B. Z.; Shih, W. K. Mater Manuf Process 1990, 5, 301.
29. Ton-That, M. T.; Cole, K. C.; Jen, C. K.; França, D. R. Polym Compos 2000, 21, 605.
30. Carlsson, L. A.; Gillespie, J. W., Eds. Delware Composites Design Encyclopedia, Vol. 3; Technomic Publishing: Lancaster, 1990.
31. Sabet, A.; Beheshty, M.; Rahimi, H. Polym Compos 2008, 29, 932.